BIOCHEMISTRY
including biophysical chemistry & molecular biology
Article

Biochemistry **2009,** *48,* 10423–10436 10423
DOI: 10.1021/bi9014242

A Library of Fluorescent Peptides for Exploring the Substrate Specificities of Prolyl Isomerases[†]

Gabriel Zoldák,[‡,⊥] Tobias Aumüller,[§,⊥] Christian Lücke,[§] Jozef Hritz,[∥] Chris Oostenbrink,[∥] Gunter Fischer,[§] and Franz X. Schmid*[,‡]

[‡]*Laboratorium für Biochemie und Bayreuther Zentrum für Molekulare Biowissenschaften, Universität Bayreuth, D-95440 Bayreuth, Germany,* [§]*Max Planck Research Unit for Enzymology of Protein Folding, Weinbergweg 22, D-06120 Halle/Saale, Germany, and* [∥]*Leiden-Amsterdam Center for Drug Research, Section of Molecular Toxicology, Department of Chemistry and Pharmacochemistry, Vrije Universiteit, De Boelelaan 1083, 1081 HV Amsterdam, The Netherlands.* [⊥]*These authors contributed equally to this work.*

Received August 14, 2009; Revised Manuscript Received September 28, 2009

ABSTRACT: To fully explore the substrate specificities of prolyl isomerases, we synthesized a library of 20 tetrapeptides that are labeled with a 2-aminobenzoyl (Abz) group at the amino terminus and a *p*-nitroanilide (pNA) group at the carboxy terminus. In this peptide library of the general formula Abz-Ala-Xaa-Pro-Phe-pNA, the position Xaa before the proline is occupied by all 20 proteinogenic amino acids. A conformational analysis of the peptide by molecular dynamics simulations and by NMR spectroscopy showed that the mutual distance between the Abz and pNA moieties in the peptides depends on the isomeric state of the Xaa−Pro bond. In the *cis*, but not in the *trans* form, there are significant chemical shift changes of the Abz and pNA moieties, because their aromatic rings are close to each other. This proximity also leads to a strong quenching of Abz fluorescence, which, in combination with a solvent jump, was used to devise a sensitive assay for prolyl isomerases. Unlike the traditional assay, it is not coupled with peptide proteolysis and thus can be employed for protease-sensitive prolyl isomerases as well. The peptide library was used to provide a complete set of P1-site specificities for prototypic human members of the three prolyl isomerase families, FKBP12, cyclophilin 18, and parvulin 14. In a second application, the substrate specificity of SlyD, a protease-sensitive prolyl isomerase from *Escherichia coli*, was characterized and compared with that of human FKBP12 as well as with homologues from other bacteria.

The *cis*−*trans* isomerization of the peptidyl−prolyl bond [prolyl isomerization (Figure 1a)] is an intrinsically slow reaction, because it involves the rotation about the peptide bond, which has partial double-bond character. Prolyl isomerizations are important rate-limiting steps in protein folding (*1*), and they are used as molecular switches to regulate the biological activity of proteins (*2*−*10*). Prolyl isomerizations are catalyzed by three distinct families of prolyl isomerases: cyclophilins, FK-506 binding proteins (FKBPs),[1] and parvulins (Figure 1b) (*11*).

The first prolyl isomerase was discovered using the modified tetrapeptide succinyl-Ala-Ala-Pro-Phe-*p*-nitroanilide (Suc-Ala-Ala-Pro-Phe-pNA) in a protease-coupled assay (*12*), which exploits the finding that α-chymotrypsin can hydrolyze the *p*-nitroanilide amide bond only when the Ala−Pro bond is in the *trans* conformation (*13*). The hydrolysis leads to an increase in absorbance at 390 nm. In aqueous solution, the assay peptide exists as a 90:10 mixture of molecules with the Ala−Pro bond in *trans* and *cis* conformations, respectively (*13*, *14*). In the presence of chymotrypsin at a high concentration, 90% of the molecules are thus cleaved rapidly, within the dead time of manual mixing. The hydrolysis of the remaining 10% is slow, because it is limited in rate by the *cis* → *trans* isomerization of the peptide, and the acceleration of this slow reaction was used as the basis for detecting and characterizing the enzymatic properties of prolyl isomerases (*12*, *15*−*17*).

This protease-coupled assay procedure, termed isomer-specific proteolysis (ISP) (*18*), has two drawbacks. The fraction of the *cis* peptide and thus the sensitivity of the assay are low, and it can be used only for prolyl isomerases that are protease-resistant. The amount of *cis* isomer and thus the sensitivity of the assay can be increased by dissolving the peptide in an anhydrous LiCl/TFE solution prior to the assay (*19*). To avoid the coupling with isomer-specific proteolysis, several variants of the peptide assay were developed (*20*−*22*). In the substrate Suc-Ala-Ala-Pro-Phe-pNA, a 1−3% change in absorbance occurs upon isomerization even in the absence of a protease. This small change was used to

[†]Supported by a DAAD postdoctoral fellowship in the program "Modern Applications of Biotechnology" (to G.Z.), by The Netherlands Organization for Scientific Research, Horizon Breakthrough Grant 935.18.018 (to J.H.), and by the Deutsche Forschungsgemeinschaft (to G.F. and F.X.S.).

*To whom correspondence should be addressed: Biochemie, Universität Bayreuth, D-95440 Bayreuth, Germany. Telephone: ++49 921 553660. Fax: ++49 921 553661. E-mail: fx.schmid@uni-bayreuth.de.

[1]Abbreviations: FKBP, FK-506 binding protein; hPar14, human parvulin 14; hCyp18, human cyclophilin 18; hFKBP12, human FKBP12; Abz, 2-aminobenzoyl; pNA, *p*-nitroaniline; ISP, isomer-specific proteolysis; PPIase, peptidyl-prolyl isomerase; Xaa, amino acid; MMIM Me_2PO_4, 1,3-dimethylimidazolium dimethylphosphate; k_{ct} and k_{tc}, microscopic rate constants for *cis*−*trans* and *trans*−*cis* isomerization reactions, respectively; K_{tc}, equilibrium constant for *cis*−*trans* isomerization; λ, macroscopic rate constant; *cis*-Pro, *cis* isomer of the Xaa−Pro peptide bond; NOESY, nuclear Overhauser enhancement spectroscopy; PDB, Protein Data Bank; rmsd, root-mean-square deviation; ROESY, rotating frame Overhauser enhancement spectroscopy; R_g, radius of gyration; HSQC, heteronuclear single-quantum coherence; TOCSY, total correlation spectroscopy.

Published on Web 09/28/2009

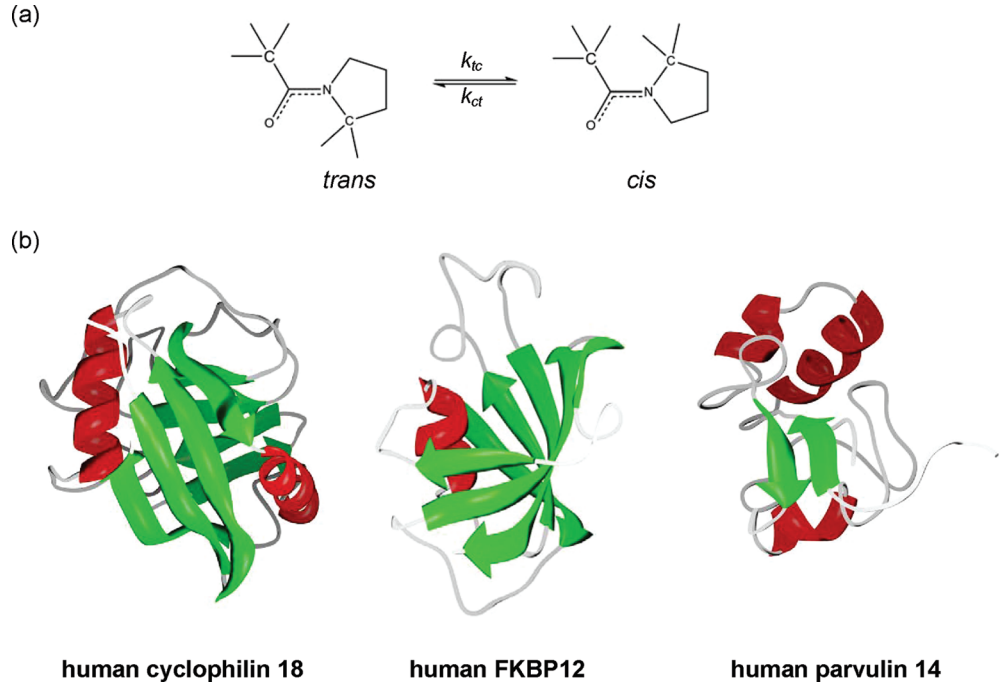

FIGURE 1: (a) *Cis*−*trans* isomerization of a Xaa−Pro bond. (b) Three-dimensional structures of representative members of the three families of prolyl isomerases, human cyclophilin 18 (PDB entry 1oca) (*66*), human FKBP12 (PDB entry 1fkf) (*67*), and human parvulin 14 (PDB entry 1fjd) (*68*). This figure was prepared using UCSF Chimera (*69*).

devise a protease-free assay (*20*). Its sensitivity is low, and it shows a poor signal-to-noise ratio. Garcia-Echeverria et al. introduced substrates that were labeled N-terminally with a 2-aminobenzoyl (Abz) residue and C-terminally with either a nitrophenylalanine residue or a 4-nitrobenzyl moiety, each of which acts as a quencher of the Abz fluorescence (*21*, *22*). The extent of quenching is different for the *cis* and *trans* forms of the peptide, and in combination with a solvent jump from a LiCl/TFE solution, this was exploited in developing a protease-free prolyl isomerase assay (*21*, *23*).

In the protease-free assays, the shift in the *cis*−*trans* equilibrium upon solvent transfer is measured, and as a consequence, the observed macroscopic rate constant is equal to the sum of the microscopic rate constants for the *cis* → *trans* (k_{ct}) and *trans* → *cis* (k_{tc}) reactions. In the protease-coupled assay, only k_{ct} is measured, because the back reaction is abolished by the rapid proteolysis of the *trans* isomer (*20*).

The substrate specificities of prolyl isomerases are determined primarily by the nature of the amino acid at the P1 position, which participates in the isomerizing peptide bond with the proline. In initial investigations of human cyclophilin 18 (hCyp18) and FKBP12, we employed limited sets of tetrapeptides and the protease-coupled assay to evaluate the substrate specificities of these prolyl isomerases, which are resistant to rapid proteolysis by chymotrypsin (*15*).

To fully explore the substrate specificities of prolyl isomerases, including those that are sensitive to proteases, we synthesized a library of 20 tetrapeptides that are labeled with an Abz group at the amino terminus and a pNA group at the carboxy terminus, which quenches the Abz fluorescence (Figure 2). In this peptide library of the general formula Abz-Ala-Xaa-Pro-Phe-pNA, the Xaa position before the proline is occupied by all 20 proteinogenic amino acids.

We first analyzed the conformations of these peptides by NMR spectroscopy and molecular dynamics simulations as well as by absorbance and fluorescence spectroscopy. The *cis*−*trans* equilibria and the isomerization kinetics were measured after jumps from different solvents to aqueous buffer. Then, this peptide library in combination with the sensitive protease-free fluorimetric assay was used to determine the substrate specificities of human members of the three PPIase families, namely, FKBP12, cyclophilin 18, and parvulin 14. In a second application, the substrate specificity of SlyD, a protease-sensitive prolyl isomerase from *Escherichia coli*, was characterized and compared with those of human FKBP12 and SlyD homologues from six other bacterial species.

MATERIALS AND METHODS

Materials. Chemical reagents and solvents were purchased from Sigma Aldrich. The amino acid derivatives, coupling reagents, and the resin were purchased from Novabiochem. The proteins hFKBP12, hCyp18, hPar14, and SlyD were purified as described previously (*16*, *24*−*26*). The peptide Suc-Ala-Glu-Pro-Phe-pNA was purchased from Bachem.

Peptide Synthesis. The Abz/pNA-tetrapeptide derivatives were synthesized employing N^{α}-9-fluorenylmethoxycarbonyl (Fmoc)-protected amino acid derivatives by manual solid-phase peptide synthesis. Trifunctional amino acids were used as the side chain-protected derivatives carrying the following side chain protection: trityl (Trt) for Gln, Asn, His, and Cys; *tert*-butyl (tBu) for Glu, Asp, Tyr, Thr, and Ser; *tert*-butyloxycarbonyl (Boc) for Lys and Trp; and 2,2,4,6,7-pentamethyldihydrobenzofuran-5-sulfonyl (Pbf) for Arg. The 2-aminobenzoic acid was introduced as the Boc-protected derivative [Abz(Boc)].

The peptides Abz(Boc)-Ala-Xaa-Pro-OH were assembled on a chlorotrityl chloride resin. After the resin had been loaded with Fmoc-Pro-OH according to the protocol given elsewhere (*27*), the peptides were elongated using activation by benzotriazol-1-yloxytrispyrrolidinophosphonium hexafluorophosphate (PyBop). Four equivalents of PyBop, 4 equiv of the Fmoc-protected amino

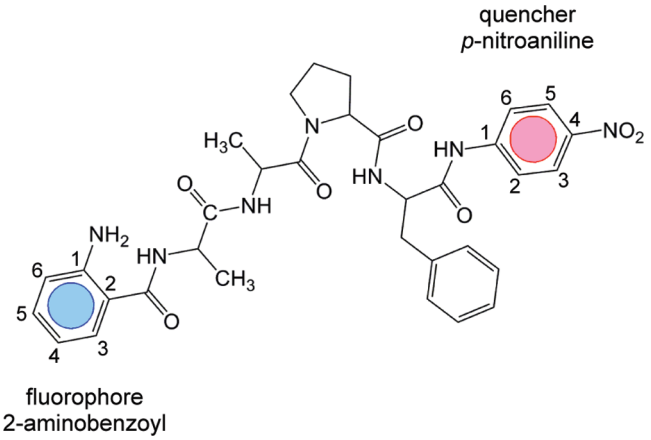

FIGURE 2: Schematic structure representation of the doubly labeled tetrapeptide Abz-Ala-Ala-Pro-Phe-pNA.

acid derivative, and 8 equiv of the auxiliary base *N*,*N*-diisopropylethylamine (DIPEA) were incubated with the resin in *N*,*N*-dimethylformamide (DMF) for 1 h at room temperature under continuous stirring to form the amide bonds. Removal of the Fmoc protection group was accomplished by incubating the resin in a 20% piperidine/DMF mixture for 15 min twice. The fully protected peptides were cleaved from the resin via application of 33% 1,1,1,3,3,3-hexafluoroisopropanol (HFIP) in dichloromethane (DCM) (*28*). Condensation of the Abz-tripeptide derivative to H-Phe-pNA HCl was conducted in tetrahydrofuran (THF) via application of 2 equiv of H-Phe-pNA HCl, 2 equiv of PyBop, and 4 equiv of DIPEA for 1 h at room temperature. Subsequently, the THF was evaporated, the crude reaction mixture dissolved in DMF, and the product precipitated by the addition of 0.3 M sodium acetate buffer (pH 5.0). The precipitate was washed with H_2O and dried overnight under vacuum. Removal of the protection groups was accomplished by treatment with a mixture of trifluoroacetic acid (TFA, 95%, v/v), triisopropylsilane (TIS, 2.5%, v/v), and H_2O (2.5%, v/v) for 1 h.

The peptide Abz-Ala-Glu-Pro-Phe-Glu-NH_2 was synthesized according to the procedure given above on a Rink amide resin. Cleavage from the resin was accomplished by treatment with a TFA (95%, v/v)/TIS (2.5%, v/v)/H_2O mixture (2.5%, v/v) for 1 h.

Finally, the peptides were purified by reversed-phase HPLC using a Hibar 250-25 LiChrospher 100 RP-8 RP column (Merck, Darmstadt, Germany). The respective sample was loaded onto the column and eluted with a linear gradient from 10 to 65% (v/v) acetonitrile (ACN) with 0.1% TFA in a H_2O/0.1% TFA mixture over 90 min at a flow rate of 16 mL/min. Fractions containing the product were combined, and the purity was checked by analytical HPLC using a gradient from 10 to 80% (v/v) ACN with 0.1% TFA in a H_2O/0.1% TFA mixture over 30 min (Grace Vydac C8 column). The identities of the products were verified by electrospray mass spectrometry (ESI-MS, Dionex, MSQ Surveyor). The yields of the isolated and purified peptides were between 20 and 40% referenced to the resin loading.

Isomer-Specific Proteolysis of the Peptides. Isomer-specific proteolysis was initiated by the addition of 240 μM α-chymotrypsin (final concentration) to 12 μM peptide in 50 mM HEPES (pH 7.8) at 15 °C and followed by the increase in absorbance at 390 nm. The fraction of the *cis* isomer in various solvents was measured after a solvent jump to 50 mM HEPES (pH 7.8) containing 240 μM α-chymotrypsin at 15 °C. The samples were stirred at a constant velocity during the measurements. The temperature was controlled with a Peltier element. Monoexponential functions were fitted to the reaction progress curves.

Fluorimetric Analysis of the Peptides and Protease-Free Assay. The assay peptides were dissolved in 50 mM HEPES (pH 7.8) in MMIM Me_2SO_4 or in an anhydrous 0.55 M LiCl/TFE mixture. Fluorescence emission spectra (3 nm bandwidth) of 1 μM Abz-peptides were measured after excitation at 316 nm (3 nm bandwidth) in 0.1 M potassium phosphate and 1 mM EDTA (pH 7.5) at 15 °C using a Jasco FP 6500 or a Hitachi F4010 spectrofluorimeter. Isomer-specific proteolysis was initiated by addition of 240 μM α-chymotrypsin (final concentration). Time courses were measured at 416 nm (3 nm bandwidth) after excitation at 316 nm (3 nm bandwidth). The samples were continuously stirred. Peptide concentrations were between 4 and 20 μM.

The protease-free assays were performed in a similar way. The reaction was initiated by a dilution of the peptide in an anhydrous 0.55 M LiCl/TFE mixture or in MMIM Me_2SO_4 with 0.1 M potassium phosphate and 1 mM EDTA (pH 7.5). Typically, these solvent jump experiments were performed as 200-fold dilutions of 600 μM peptide stock solutions. Time courses were measured at 416 nm (5 nm bandwidth) after excitation at 316 nm (3 nm bandwidth).

For all peptides, the *cis*−*trans* isomerization reactions were independent of the peptide concentration at concentrations of < 5 μM and followed monoexponential time courses. At high peptide concentrations (> 10 μM) and high salt concentrations (> 0.5 M NaCl), several hydrophobic peptides exhibited more complicated kinetics, probably because isomerization was accompanied by aggregation.

The *cis*−*trans* isomerization reaction could be followed in several widely used buffers (Tris, HEPES, MOPS, and cacodylate), in the presence of denaturants such as urea or GdmCl, in the presence of redox reagents such as TCEP or DTT, in the presence of metal ions (Ni^{2+}, Co^{2+}, and Mg^{2+}), and even in turbid media, demonstrating that the solvent jump assay is robust and can be used under widely differing conditions.

The quantum yield Φ of Abz-Ala-Glu-Pro-Phe-Glu-NH_2 in 0.1 M potassium phosphate buffer (pH 7.5) at 10 °C was calculated from the integrated emission intensity (λ_{ex} = 316 nm; OD_{316} = 0.01) using 1,4-bis(5-phenyloxazol-2-yl)benzene in cyclohexane (Φ_{ref} = 0.97) (*29*) as a standard. The Φ value was corrected for refractive index variation of sample and reference (*30*). The Förster distance R_0 was calculated using a κ^2 of $^2/_3$, an ε_{315} of 14000 M^{-1} cm^{-1} (*31*), and a refractive index of 1.34 (*32*).

Protease-Free PPIase Assay. Peptide (~0.5 mg) was dissolved in 1 mL of an anhydrous 0.55 M LiCl/TFE solvent mixture and stored at 4 °C in an exsiccator filled with hygroscopic material (silica gel, P_2O_5 powder). Solvent jumps were initiated by addition of the 5 μL aliquot of the 750 μM peptide stock solution in a 0.55 M LiCl/TFE mixture to 995 μL of 0.1 M potassium phosphate and 1 mM EDTA (pH 7.5) in a fluorescence cell in the absence and presence of PPIase. Fluorescence at 416 nm was measured after excitation at 316 nm. The time courses of the *cis*−*trans* isomerization were analyzed as single-exponential reactions, and the apparent rate constants are plotted as a function of enzyme concentration. The time course of the reaction is described by the rate constant $k_{app} = k_0 + [E] \times k_{cat}/K_M$, where k_0 is the rate constant of the uncatalyzed reaction, [E] is the enzyme concentration, and k_{cat} and K_M are the turnover

number and the Michaelis constant, respectively. A plot of k_{app} versus enzyme concentration gives a slope equal to the catalytic efficiency, k_{cat}/K_M.

NMR Measurements. The NMR samples generally contained 2−2.5 mM peptide in 100 mM potassium phosphate buffer (pH 7.5, 5% D_2O). Standard one-dimensional (1D) and two-dimensional (2D) ($^1H-^1H$ TOCSY, $^1H-^1H$ NOESY, $^1H-^1H$ ROESY, and $^1H-^{13}C$ HSQC) pulse sequences were employed to collect data at 10 °C with a Bruker DMX 500 spectrometer operating at a proton resonance frequency of 500.13 MHz and equipped with a 5 mm triple-resonance $^1H\{^{13}C/^{15}N\}$ probe that had *XYZ* gradient capability. The data were collected with the carrier placed in the center of the spectrum on the water resonance, which was suppressed by presaturation or gradient pulses. Quadrature detection in the indirectly detected dimension of 2D experiments was achieved by the States−TPPI or echo−antiecho method. TOCSY spectra were collected with 80 and 6 ms spin-lock times and NOESY and ROESY spectra with 300 and 225 ms mixing times, respectively. All NMR spectra were acquired, processed, and analyzed on Silicon Graphics computers using XWINNMR version 3.5 (Bruker Bio-Spin, Rheinstetten, Germany). A 90° phase-shifted squared sine-bell function was used for apodization in all dimensions. Polynomial baseline correction was applied to the processed spectra in the directly detected ^1H dimension. The chemical shifts were referenced to external DSS to ensure consistency among all spectra (*33*, *34*).

Molecular Dynamics Calculations. Initial conformations of the peptides Abz-Ala-Xaa-Pro-Phe-pNA (Xaa is Gly, Ala, or Glu) with Pro in either the *trans* or the *cis* conformation were generated in MOE (*35*). The molecular dynamics study was performed using the GROMOS05 simulation package (*36*) in combination with the GROMOS-53A6 force field (*37*). Force field parameters used for uncommon parts of the Abz and pNA end groups were prepared individually and implemented in the GROMOS05 simulation package (Tables S1 and S2 of the Supporting Information). All bonds were constrained, using the SHAKE algorithm (*38*) with a relative geometric accuracy of 10^{-4}, allowing for a time step of 2 fs used in the leapfrog integration scheme (*39*). Rectangular periodic boundary conditions were applied. After a steepest descent minimization to remove bad contacts between molecules, initial velocities were randomly assigned from a Maxwell−Boltzmann distribution at 300 K, according to the atomic masses. The temperature was kept constant using weak coupling to a bath of 300 K with a relaxation time of 0.1 ps (*40*). The peptide and the solvent [2012 explicit SPC (*41*) water molecules] were independently coupled to the heat bath. The pressure was controlled using isotropic weak coupling to atmospheric pressure with a relaxation time of 0.5 ps (*40*). van der Waals and electrostatic interactions were calculated using a triple-range cutoff scheme. Interactions within a short-range cutoff of 0.8 nm were calculated every time step from a pair list that was generated every five steps. At these time points, interactions between 0.8 and 1.4 nm were also calculated and kept constant between updates. A reaction field contribution was added to the electrostatic interactions and forces to account for a homogeneous medium outside the long-range cutoff, using the relative permittivity of 61 of SPC water (*42*). The system was equilibrated for 2 ns, and the length of the production run was 120 ns. Coordinates of atoms were stored every 4 ps. Cluster analysis of peptides was performed using gromos++ tool *cluster* (*43*) with a rmsd cutoff of 0.25 nm.

Table 1: Chemical Shift Values (in parts per million) for the Abz and pNA Ring Protons (Figure 2) of the Peptides Abz-Ala-Glu-Pro-Phe-pNA, Suc-Ala-Glu-Pro-Phe-pNA, and Abz-Ala-Glu-Pro-Phe-Glu-NH_2[a]

	Abz moiety				pNA moiety	
peptide	H3	H4	H5	H6	H2/H6	H3/H5
Abz-Ala-Glu-Pro-Phe-pNA						
trans-Pro	7.52	6.85	7.34	6.88	7.50	8.21
cis-Pro	7.34	6.72	7.25	6.76	7.39	8.08
Suc-Ala-Glu-Pro-Phe-pNA						
trans-Pro	–	–	–	–	7.49	8.21
cis-Pro	–	–	–	–	7.52	8.22
Abz-Ala-Glu-Pro-Phe-Glu-NH_2						
trans-Pro	7.50	6.85	7.35	6.89	–	–
cis-Pro	7.52	6.85	7.35	6.89	–	–

[a]The ^1H chemical shift values were obtained from $^1H-^1H$ TOCSY spectra collected with a spin-lock time of 80 ms. Measurements were performed at 10 °C using 2−2.5 mM peptide dissolved in 100 mM potassium phosphate buffer (pH 7.5, 5% D_2O).

RESULTS AND DISCUSSION

Conformational Analysis by NMR Spectroscopy. The conformation of the doubly labeled peptide Abz-Ala-Glu-Pro-Phe-pNA was analyzed by one- and two-dimensional NMR spectroscopy. The respective ^1H and ^{13}C resonance assignments are listed in Table S3 of the Supporting Information. Individual sets of resonances were identified for the *trans*-Pro form and the *cis*-Pro form of the peptide. The different proline conformers could be discerned on the basis of NOE and ROE connectivities between the Hα atom of the preceding glutamate and either the Hα or Hδ atom(s) of the proline residue (*44*) and on the basis of the characteristic ^{13}C chemical shift values of the proline Cβ and Cγ nuclei (*45*). Furthermore, the apparent lack in the NOESY and ROESY spectra of dipolar couplings between the Abz and pNA ring moieties implies that the average distance between the Abz and pNA moieties is >5 Å. In the *cis*-Pro form, the ^1H resonances of the Abz and pNA ring protons are shifted upfield by 0.1−0.2 ppm, compared to those of the *trans*-Pro form (Table 1), suggesting that the isomeric state of the proline influences the chemical environment of the two fluorophores (Figure 3). The phenylalanine ring is hardly affected by the proline conformation, and only a minor chemical shift change of 0.04 ppm was observed for the Hζ resonance. The *cis*:*trans* ratio in the doubly labeled peptide was 0.22:0.78, as determined from an integration of the pNA H3/H5 signals in the 1D spectrum.

NMR spectra were also recorded for two control peptides that lacked either the Abz moiety (Suc-Ala-Glu-Pro-Phe-pNA) or the pNA moiety (Abz-Ala-Glu-Pro-Phe-Glu-NH_2). The corresponding ^1H and ^{13}C resonances are listed in Tables S4 and S5 of the Supporting Information, respectively. In both control peptides, the remaining chromophore (Abz or pNA) exhibited virtually identical chemical shift values in the *trans*-Pro form and the *cis*-Pro form (Table 1); moreover, these chromophore resonances coincided with the ones obtained for the *trans* form of the doubly labeled peptide (Figure 3). This resonance congruence indicates that, in the *trans*-Pro form of the doubly labeled peptide, the chemical environment of each chromophore is not affected by the respective other chromophore, because they are remote from each other.

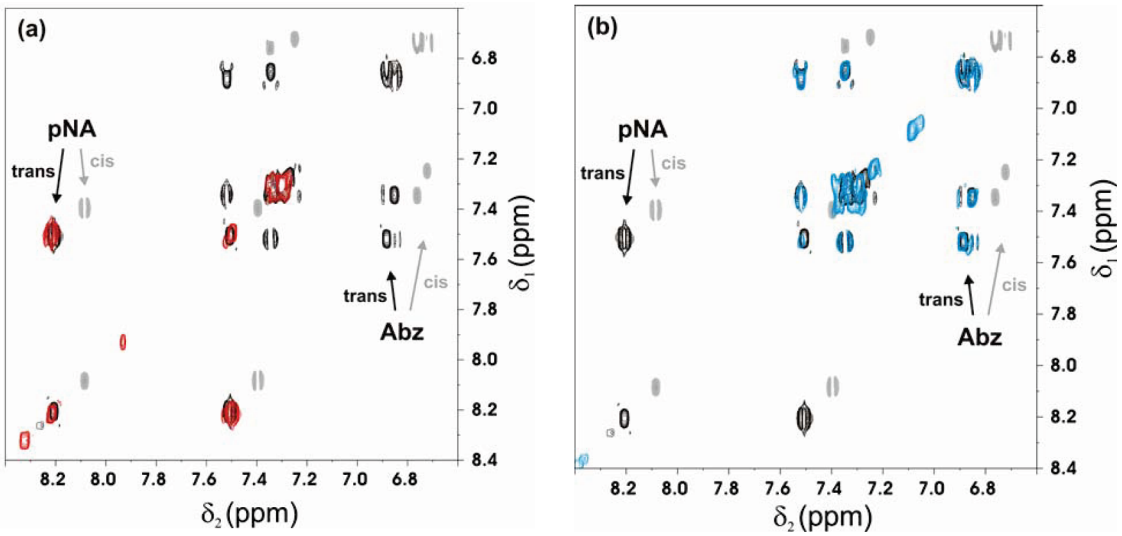

FIGURE 3: (a) Overlay of the aromatic regions of the $^1H-^1H$ TOCSY spectra of Abz-Ala-Glu-Pro-Phe-pNA (black/gray contours) and Suc-Ala-Glu-Pro-Phe-pNA (red contours), showing the congruence of the signals that represent the Abz ring protons of Suc-Ala-Glu-Pro-Phe-pNA and of the *trans*-Pro form (black contours) of Abz-Ala-Glu-Pro-Phe-pNA. In the *cis*-Pro form (gray contours) of Abz-Ala-Glu-Pro-Phe-pNA, the fluorophore signals are all shifted upfield relative to the control, indicating a parallel stacking interaction between the Abz and pNA ring planes. (b) Overlay of the aromatic regions of the $^1H-^1H$ TOCSY spectra of Abz-Ala-Glu-Pro-Phe-pNA (black/gray contours) and Abz-Ala-Glu-Pro-Phe-Glu-NH_2 (cyan contours). Again, the signals of the Abz ring protons in Abz-Ala-Glu-Pro-Phe-Glu-NH_2 coincide with those of the *trans*-Pro form (black contours) of Abz-Ala-Glu-Pro-Phe-pNA, while the cross-peaks of the Abz-Ala-Glu-Pro-Phe-pNA *cis*-Pro form (gray contours) are all shifted upfield.

The pronounced upfield shifts observed for resonances of the *cis*-Pro isomer (relative to the *trans*-Pro form) of the doubly labeled peptide, on the other hand, originate from mutual ring current effects between the Abz and pNA moieties. Such effects require ring-to-ring distances of <7 Å, suggesting that, in the *cis*-Pro form, the Abz and pNA ring planes can approach each other at such a short distance in an approximately parallel fashion. At the same time, the above-mentioned lack of both NOE and ROE connectivities between the chromophores, in the *cis*-Pro form of the doubly labeled peptide, implies that the Abz and pNA rings are on average more than 5 Å apart. Hence, an average inter-ring distance of 5−7 Å can be assumed in the *cis*-Pro form, whereas the distance between the two rings is apparently larger in the *trans*-Pro form.

Molecular Dynamics Simulations of the Doubly Labeled Peptides. The conformational dynamics of the doubly labeled peptide Abz-Ala-Glu-Pro-Phe-pNA was also analyzed by molecular dynamics simulations for the *trans* form and the *cis* form. Both can adopt wide ranges of conformations, indicating that, overall, the peptides are unstructured. Nevertheless, the statistical analysis of the entire ensembles of structures (Figure 4) reveals pronounced differences between the two forms of the peptide. The *cis* isomer exists partially in a closed form, and the distribution of the distances between the centers of the terminal chromophores shows a narrow peak around 5 Å (Figure 4a) for ~46% of all molecules. The remaining molecules show more extended conformations (Figure 4). In contrast, the *trans* isomer exists mostly in an extended conformation in which the centers of the chromophoric groups are approximately 18 Å from each other. The different intramolecular distance distributions for the two forms of the peptide (Figure 4a) are also reflected in different average radii of gyration (Figure 4b).

Similar distance distributions (Figure 4c) and radii of gyration (Figure 4d) were also found for the *cis* and *trans* forms of the peptide in which Pro is preceded by Ala (Abz-Ala-Ala-Pro-Phe-pNA). Representative structures of the *cis* and *trans* isomers of the peptides in different conformations are shown in Figure S1 of the Supporting Information. The *cis* isomer shows two alternative conformations (Figure S1ab), while the *trans* isomer predominates in a single conformation (Figure S1c). Different

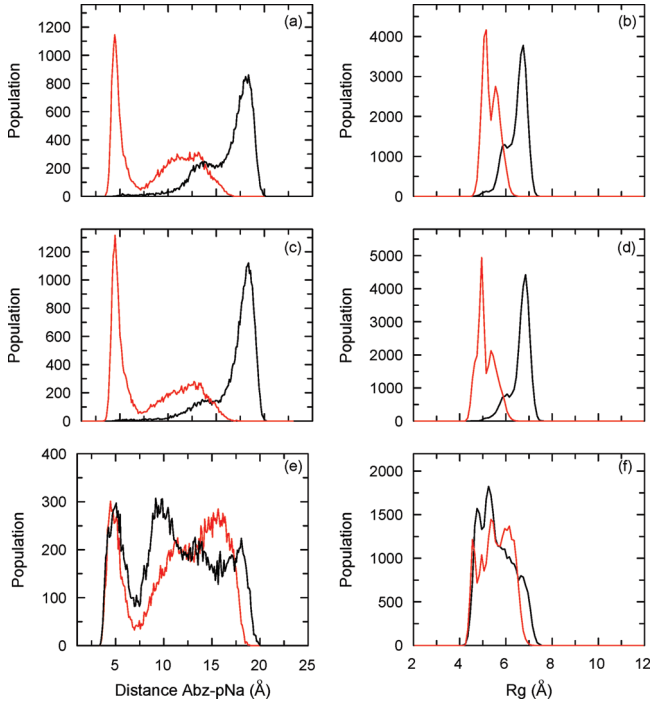

FIGURE 4: (a, c, and e) Distribution of the distances between the centers of mass of the aromatic rings of the Abz and pNA moieties for the *cis* (red curves) and *trans* isomers (black curves) for Abz-Ala-Xaa-Pro-Phe-pNA peptides: (a) Xaa = Glu, (c) Xaa = Ala, and (e) Xaa = Gly. (b, d, and f) Distribution of the radii of gyration for the *cis* (red curves) and *trans* isomers (black curves) for Abz-Ala-Xaa-Pro-Phe-pNA peptides: (b) Xaa = Glu, (d) Xaa = Ala, and (f) Xaa = Gly. The distributions were calculated from the time series of the distances and gyration radii of the simulated peptides. They were obtained from molecular dynamics simulations as described in Materials and Methods.

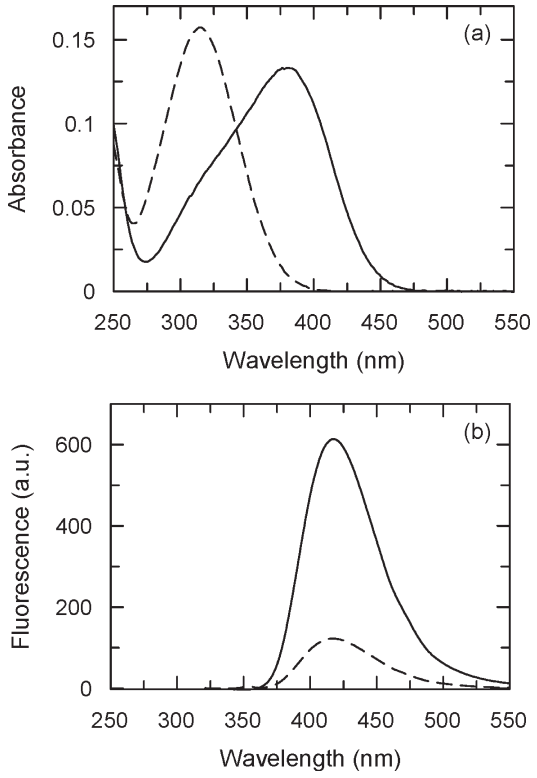

FIGURE 5: (a) Absorbance and (b) fluorescence spectra of the Abz-Ala-Glu-Pro-Phe-pNA peptide before (– – –) and after (—) proteolysis by 24 μM α-chymotrypsin. The spectra of α-chymotrypsin were subtracted. The absorbance spectra were measured with 10 μM peptide and the fluorescence spectra with 1 μM peptide, both in 50 mM Hepes (pH 7.8) at 15 °C.

results were obtained when Pro was preceded by Gly (in the Abz-Ala-Gly-Pro-Phe-pNA peptide). In this case, broad distance distributions were found, which are similar for the *cis* and the *trans* forms of the peptide (Figure 4e), indicating that the inherently high backbone flexibility at Gly residues compensates for the differences in the static bending of the backbone at the Gly−Pro bond. Moreover, the two isomers of the Gly peptide exhibited nearly the same average radii of gyration (Figure 4f).

In the MD simulations, a significant fraction of molecules with end group distances of < 5 Å is observed only for the *cis* isomers (Figure 4). This agrees well with the NMR result that the chemical shifts of the chromophores affect each other in the *cis* but not in the *trans* forms of the peptides (*72*).

Spectral Properties of the Labeled Peptides. The doubly labeled tetrapeptides exhibit nearly identical absorbance spectra with a maximum at 315 ± 2 nm, which originates predominantly from the pNA group. The spectrum for Abz-Ala-Glu-Pro-Phe-pNA is shown in Figure 5a. The cleavage by α-chymotrypsin leads to the release of *p*-nitroaniline and to a corresponding bathochromic shift of the pNA absorption band by 65 nm. This shift and the comparison with the spectrum of *p*-nitroaniline allowed us to calculate the contribution of the Abz group to the absorbance spectra of the peptides before and after proteolysis. It indicates that, in the doubly labeled peptides, only ~20% of the absorbance at 316 nm originates from the Abz moiety.

The fluorescence spectra of the doubly labeled peptides showed a maximum near 420 nm (after excitation at 316 nm), as shown for Abz-Ala-Glu-Pro-Phe-pNA in Figure 5b. The fluorescence intensity increased strongly (5−6-fold) upon proteolytic removal of the pNA group, which indicates that, in the doubly labeled peptides, the Abz fluorescence is strongly quenched. The spectral overlap between the emission band of the Abz group and the absorption band of the pNA group is rather small but allows, in principle, Förster resonance energy transfer. The quantum yield of the Abz moiety in the absence of the quencher has been determined ($\Phi_{Abz} = 0.48 \pm 0.04$) using the Abz-Ala-Glu-Pro-Phe-Glu-NH_2 peptide and 1,4-bis(5-phenyloxazol-2-yl)benzene in cyclohexane ($\Phi_{ref} = 0.97$) as a standard (*29*). The Förster distance calculated from the spectra is ~16 Å (using a κ^2 of $^2/_3$ and a refractive index of 1.34). The average intramolecular distances between the two chromophores, as calculated from the molecular dynamics simulations (~18 Å for the *trans* form and ~5 Å for the *cis* form), are both within the range suitable for energy transfer, suggesting that it contributes to the observed strong reduction of the Abz fluorescence in the doubly labeled peptides. An additional decrease in Abz fluorescence originates probably from dynamic or static quenching by the pNA moiety (*46*).

The strong increase in fluorescence upon cleavage at a high protease concentration provides a straightforward method for following the kinetics of the *cis*−*trans* isomerization. The extent of intramolecular quenching depends on the *cis*:*trans* ratio at the Xaa−Pro bond, and as described later, solvent jump experiments monitored by fluorescence can be used to follow the *cis*−*trans* isomerization in the intact peptides.

Measurement of the Cis−*Trans Xaa*−*Pro Equilibria in the Peptide Library by Isomer-Specific Proteolysis*. The Abz peptides in our library were designed such that they could be employed for both the protease-free fluorescence assay and the isomer-specific proteolysis (ISP) assay with α-chymotrypsin (*12*, *13*, *18*). Proteolysis of the *trans* peptide by 240 μM α-chymotrypsin, as measured by the increase in *p*-nitroaniline absorbance at 390 nm, is complete within the dead time of mixing, as shown in Figure 6a for the Ala peptide. At this α-chymotrypsin concentration, there is no cleavage of the *cis* isomer. Consequently, the second slow phase is limited in rate by the *cis* → *trans* isomerization, and its amplitude reflects the fraction of the molecules with a *cis* prolyl bond, as present before the proteolysis.

Prior to ISP, the peptides were equilibrated in aqueous buffer [0.1 M potassium phosphate (pH 7.5)] or in a 0.55 M LiCl/TFE mixture. The preincubation of the doubly labeled Ala peptide in the different solvents had virtually no effect on the time course of *cis* → *trans* isomerization after dilution into aqueous buffer. All time courses were described well by single-exponential functions, giving time constants of 77 and 72 s for the cleavage of the peptide after preincubation in aqueous buffer or in a 0.55 M LiCl/TFE mixture. Increasing the concentration of α-chymotrypsin to 480 μM also had no effect on the amplitudes and rates of the slow reaction in the ISP assay. The solvents affected the *cis*−*trans* equilibrium differently, and as a consequence, the slow phase in isomer-specific proteolysis showed amplitudes different in magnitude (Figure 6). The analysis of these amplitudes provides a simple and direct means of determining the *cis*−*trans* equilibria in the different solvents for the peptides. For the Ala peptide (Figure 6), *cis* isomer contents of 20 and 41% were derived after incubation in aqueous buffer and a 0.55 M LiCl/TFE mixture, respectively. This confirms that the *cis* isomer content is significantly increased in the presence of the LiCl/TFE mixture (*19*).

Upon cleavage by chymotrypsin, the two chromophores become fully separated, and the fluorescence intensity of the Abz moiety increases strongly. This increase provides an extremely sensitive probe for following the kinetics of *cis* → *trans* isomerization by ISP with a high signal-to-noise ratio, even at

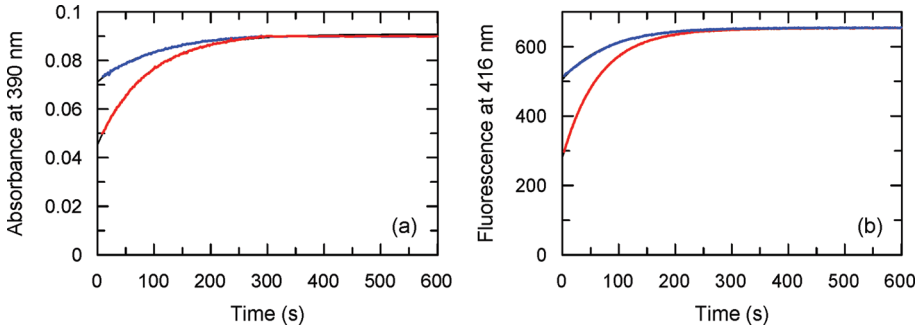

FIGURE 6: Time dependence of (a) the absorbance at 390 nm and (b) the fluorescence at 416 nm after excitation at 316 nm of Abz-Ala-Ala-Pro-Phe-pNA during the cleavage by 240 μM α-chymotrypsin in 0.1 M potassium phosphate and 1 mM EDTA (pH 7.5) at 15 °C. The peptide concentration was 7 μM for absorbance and 1 μM for fluorescence measurements. Prior to proteolysis, the peptide was dissolved in 0.1 M potassium phosphate, 1 mM EDTA buffer (pH 7.5) (blue curve) or in a 0.55 M LiCl/TFE mixture (red curve). The cleavage of the *trans* isomer is complete within the first 10 s and not visible in the figures. The lines represent monoexponential functions that were fitted to the data by nonlinear regression. The absorbance kinetics in panel a give the following rate constants: $\lambda = 0.011\ s^{-1}$ (blue), and $\lambda = 0.012\ s^{-1}$ (red). The fluorescence kinetics in panel b give the following rate constants: $\lambda = 0.012\ s^{-1}$ (blue). and $\lambda = 0.015\ s^{-1}$ (red).

Table 2: Equilibrium and Kinetic Properties of the *Cis*−*Trans* Isomerization Reactions of the Doubly Labeled Peptides

	ISP LiCl/TFE[a]	ISP buffer[b]				protease-free,[c] 0.55 M LiCl/TFE → buffer	
residue Xaa	*cis* content (%)	*cis* content (%)	k_{ct}[d] (s^{-1})	k_{tc}[e] (s^{-1})	$\lambda = k_{tc} + k_{ct}$[f] ($s^{-1}$)	λ[g] (s^{-1})	amplitude[h] (%)
Ala	41 ± 3	21 ± 1	0.012	0.0032	0.015	0.012	43
Cys	26 ± 1	13 ± 1	0.014	0.0021	0.016	0.021	7.3
Asp	11 ± 1	19 ± 1	0.0070	0.0017	0.0090	0.0083	−1.6
Glu	41 ± 3	22 ± 1	0.0074	0.0021	0.0095	0.0081	27
Phe	72 ± 3	53 ± 2	0.0069	0.0078	0.015	0.016	72
Gly	13 ± 1	13 ± 2	0.022	0.0033	0.025	0.022[i]	−11[i]
His	17 ± 1	33 ± 2	0.018	0.0089	0.027	0.021	5.2
Ile	43 ± 3	19 ± 1	0.0087	0.0021	0.011	0.010	28
Lys	28 ± 1	17 ± 1	0.016	0.0032	0.019	0.013	30
Leu	50 ± 1	10 ± 1	0.018	0.0020	0.020	0.013	20
Met	61 ± 3	36 ± 2	0.011	0.0062	0.017	0.015	36.7
Asn	7 ± 1	12 ± 1	0.016	0.0022	0.018	0.016	3.5
Pro	95 ± 1	40 ± 1	0.0027	0.0018	0.0045	0.0043	59
Gln	43 ± 1	19 ± 1	0.011	0.0026	0.014	0.012	61
Arg	55 ± 1	16 ± 1	0.013	0.0026	0.016	0.026	50
Ser	8 ± 1	21 ± 2	0.0069	0.0018	0.009	0.011	−4
Thr	9 ± 1	16 ± 2	0.025	0.0048	0.030	0.026	−2.3
Val	39 ± 1	16 ± 1	0.010	0.0019	0.012	0.0081	30
Tyr	66 ± 1	51 ± 2	0.0091	0.0095	0.019	0.014	68
Trp	80 ± 2	61 ± 2	0.0034	0.0053	0.010	0.011	8

[a]The *cis* contents were obtained from the relative amplitude of the slow proteolysis reaction in ISP experiments as described in the legend of Figure 6a. Before the proteolysis reaction, the peptides were incubated in a 0.55 M LiCl/TFE mixture. [b]Data obtained after incubation of the peptides in 50 mM HEPES buffer (pH 7.8) followed by ISP under the same conditions. [c]Data obtained after incubation of the peptides in a 0.55 M LiCl/TFE mixture followed by the protease-free solvent jump experiment and monitored by the change in Abz fluorescence. [d]The rate constant k_{ct} for *cis*−*trans* isomerization in buffer was measured directly. [e]The rate constant k_{tc} for the *trans*−*cis* isomerization was calculated from k_{ct} and K_{eq} ($=k_{tc}/k_{ct}$). [f]The calculated macroscopic rate constant $\lambda = k_{tc} + k_{ct}$ from ISP assays. [g]Apparent rate constants as measured in the protease-free assay (e.g., Figure 8a). [h]The amplitudes measured after the solvent jump from a 0.55 M LiCl/TFE mixture to buffer relative to the final fluorescence value. [i]Rate constant and amplitude obtained after a solvent jump from MMIM Me_2PO_4 to buffer.

a very low peptide concentration (Figure 6b). The rates of isomerization were identical with those measured by *p*-nitroaniline absorbance (Figure 6a), and there was a good correlation between the relative amplitudes obtained by absorbance or fluorescence after incubation of the peptide in aqueous buffer or in a 0.55 M LiCl/TFE mixture. The relative concentrations of the *cis* and *trans* isomers can be calculated more easily, however, from the absorbance measurements because, in the analysis of the fluorescence data, the different quantum yields of the Abz group in the *cis* and *trans* isomers must be included.

We used preincubation in aqueous buffer or in a 0.55 M LiCl/TFE mixture and the ISP assay based on absorbance measurements to determine the *cis* contents for all peptides of our library. The results are listed in Table 2 and shown in Figure 7. High *cis* isomer contents were found for the peptides in which Pro was preceded by an aromatic residue, in particular in the presence of a 0.55 M LiCl/TFE mixture (up to 80% *cis* for the Trp peptide). For most peptides, the *cis* content was higher in a 0.55 M LiCl/TFE mixture than in aqueous buffer. Particularly strong increases were observed for the aliphatic residues and for Arg and Glu, but not for Asp. For polar side chains such as Ser, Thr, Asn, and His, the *cis* content was lowered in the presence of a 0.55 M LiCl/TFE mixture.

Interestingly, the Gly peptide shows the same *cis*:*trans* ratio in the 0.55 M LiCl/TFE mixture and in aqueous buffer. Thus, a jump between the two solvents cannot be used to measure the

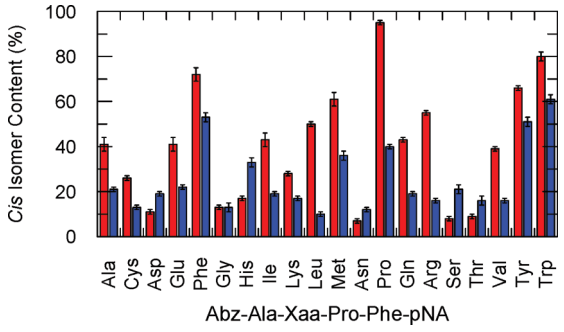

FIGURE 7: *Cis* isomer contents of the Abz-Ala-Xaa-Pro-Phe-pNA peptides in 50 mM HEPES (pH 7.8) (blue bars) or in a 0.55 M LiCl/TFE mixture (red bars) at 15 °C. The abscissa shows the nature of residue Xaa in the peptide. The content of the *cis* isomer was calculated from the amplitude of the slow reaction in isomer-specific proteolysis reactions with 240 μM α-chymotrypsin. The measurements were performed as described in the legend of Figure 6a. For Abz-Ala-Pro-Pro-Phe-pNA, only apparent values are given, because two different *cis*−*trans* isomerization equilibria can occur resulting in four different molecular species (*48*).

isomerization of this peptide. Possibly, the interactions of the solvent are identical for the *cis* and *trans* isomers of the Gly peptide, as suggested by the molecular dynamics simulations, which indicated that the *cis* and *trans* isomers of the Gly peptide have nearly the same compactness (Figure 4f) and accessible surface area (data not shown).

Recently, the ionic liquid 1,3-dimethylimidazolium dimethylphosphate (MMIM Me_2PO_4) has been shown to affect the prolyl *cis*−*trans* equilibrium in peptides, thus providing an alternative to using a LiCl/TFE mixture (*47*). Accordingly, the doubly labeled Gly peptide was dissolved in pure MMIM Me_2PO_4 and then transferred to aqueous buffer for the ISP assay. This preincubation of the peptide in the ionic liquid solvent had virtually no effect on the rate of *cis* → *trans* isomerization after dilution into aqueous buffer, but it enhanced the percentage of the *cis* isomer from 13% (as in aqueous buffer) to 37% (Table S6 of the Supporting Information). Similar measurements were also performed for the peptides with Asn, Glu, or Ala before proline. In these peptides, the percentage of the *cis* isomer is decreased in the presence of the ionic liquid (Table S6 of the Supporting Information). Apparently, interactions with the ionic liquid can shift the *cis*−*trans* equilibrium distribution in either direction depending on the amino acid preceding the proline residue.

Generally, the doubly labeled peptides of our library exhibited higher *cis*-Pro contents than the unlabeled more hydrophilic pentapeptides Ac-Ala-Xaa-Pro-Ala-Lys-NH_2 as used in the work of Reimer et al. (*48*) (Figure S2 of the Supporting Information) or in a protein Xaa−Pro library (*49*). The differences do not follow a simple correlation, suggesting that several factors might contribute. When only the Abz moiety was removed or replaced by the more hydrophilic succinyl group (in Suc-Ala-Ala-Pro-Phe-pNA), the percentage of *cis* isomer was also decreased (*23*). This suggests that weak interactions between the chromophores and, possibly, the Phe residue of the peptide slightly strengthen the preference for the *cis* isomer.

Cis−*Trans Isomerization after Solvent Jumps in the Absence of a Protease*. For most peptides of the library, the *cis* content was higher in the LiCl/TFE mixture than in aqueous buffer (see Figure 7 and Table 2). A shift in the *cis*−*trans* equilibrium was therefore induced by a solvent jump from the LiCl/TFE mixture to aqueous buffer in the absence of a protease,

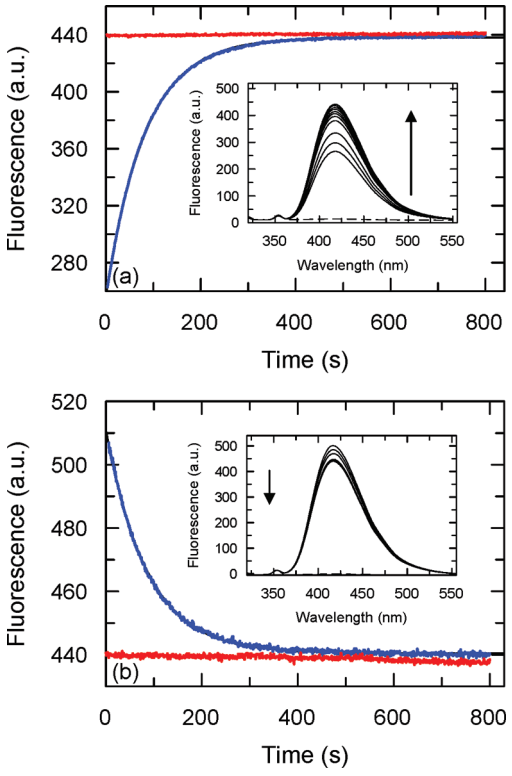

FIGURE 8: Solvent jump experiments for Abz-Ala-Ala-Pro-Phe-pNA from (a) an anhydrous 0.55 M LiCl/TFE mixture or (b) neat MMIM Me_2PO_4 to 0.1 M potassium phosphate and 1 mM EDTA (pH 7.5) at 15 °C in the absence of α-chymotrypsin, initiated by a 200-fold dilution from 600 to 3 μM peptide. The blue traces in panels a and b show the time courses of the fluorescence at 416 nm after excitation at 316 nm, and the red traces show the fluorescence after the completion of *cis*−*trans* equilibration. The equilibration reactions show identical apparent rate constants (λ) of 0.012 s^{-1} in panels a and b. The inset in panel a shows the emission spectra 5 (bottom curve), 30, 60, 110, 140, 170, 190, 220, 250, 340, and 450 s (top curve) after the solvent jump. The inset in panel b shows the emission spectra at 5 (top curve), 30, 60, 120, 180, 370, and 480 s (bottom curve). The buffer fluorescence is shown by the dashed lines.

and the corresponding change in Abz fluorescence was used to monitor this reaction with high sensitivity. The measured rate of this relaxation process, λ, is equal to the sum of the microscopic rate constants, k_{ct} for the *cis* → *trans* reaction and k_{tc} for the *trans* → *cis* reaction. Figure 8a shows the increase in fluorescence of the Ala peptide after the solvent jump from the LiCl/TFE mixture to aqueous buffer and its time course. The increase in emission intensity is smaller than in the ISP assay with α-chymotrypsin; however, the signal-to-noise ratio is high, and the signal remains constant after the reaction.

In MMIM Me_2PO_4, the *cis* content of the Ala peptide is lower than in aqueous buffer (Table S6 of the Supporting Information). Accordingly, it increased upon solvent transfer, and the fluorescence intensity decreased (Figure 8b). The time constants measured for *cis*−*trans* equilibration after the solvent jumps from the LiCl/TFE mixture (84 s) or from MMIM Me_2PO_4 (86 s) are virtually identical, and the Abz fluorescence remained constant after the reaction as well. The time constants and relative amplitudes of isomerization were found to be independent of the peptide concentration between 1 and 10 μM (data not shown).

Solvent jump experiments as described in the legend of Figure 8 were performed for all 20 peptides, and the results are summarized in Table 2. In contrast to a solvent jump from a 0.55 M LiCl/TFE mixture, a solvent jump from MMIM Me_2PO_4 to aqueous

buffer allows measurement of the *cis*−*trans* isomerization of the Abz-Ala-Gly-Pro-Phe-pNA peptide as the fraction of *cis* isomer is increased in this solvent (Table S6 of the Supporting Information). The apparently slowest isomerizations occurred for Pro−Pro (τ = 235 s at 15 °C) and Glu−Pro (τ = 123 s at 15 °C) bonds. On the other hand, Gly, Cys, Arg, Thr, and His peptides (Table 2) isomerize rather rapidly with time constants of 38−45 s. The amplitudes of isomerization varied between −4 and 72% of the final fluorescence value. The highest amplitudes were observed for aromatic and nonpolar amino acids. Generally, the Abz fluorescence increased when the fraction of the *cis* isomer decreased after the solvent jump (Table 2), because the intramolecular quenching by the pNA group becomes less efficient. A notable exception is provided by the His peptide. Here an increase in the fraction of the *cis* isomer is accompanied by an increase in fluorescence intensity (Table 2). The magnitude of the observed reaction amplitudes depends primarily on the change in the *cis*:*trans* ratio and on the difference in quantum yield between the two isomers. The correlation between the relative amplitude and the change in *cis* isomer population seems to be the major factor, and the respective Pearson correlation coefficient is 0.68. It improves to 0.83 when the aromatic residues and histidine are excluded. The observed rate constants λ from the solvent jump experiment in the absence of protease agree well with those obtained from the ISP assays (Table 2).

Prolyl Isomerase Activities Measured by the Protease-Free and Protease-Coupled Assays. Our doubly labeled peptides are suitable as substrates for both the protease-coupled and protease-free prolyl isomerase assay. Figure 9a compares the activities of human FKBP12 as measured by these two assays and by using the Leu peptide as the substrate. FKBP12 is resistant toward cleavage by chymotrypsin, and therefore, the catalytic efficiency in the protease-coupled assay (k_{cat}/K_M = 1.6×10^6 M^{-1} s^{-1}) is similar to the efficiency measured in the protease-free assay (k_{cat}/K_M = 2.3×10^6 M^{-1} s^{-1}).

The prolyl isomerase activities of two SlyD homologues were also determined. SlyD is a bacterial FKBP-type prolyl isomerase (*25*, *50*−*54*). The enzyme from the thermophilic organism *Thermus thermophilus* showed similar activities in the two assays (Figure 9b), evidently because this SlyD protein is thermostable and protease-resistant. Under the same conditions, SlyD from the mesophilic organism *E. coli* was inactive in the protease-coupled assay (Figure 9c). The same observation had been reported previously (*20*, *51*). In the protease-free assay, however, SlyD from *E. coli* shows an activity (k_{cat}/K_M = 2.8×10^6 M^{-1} s^{-1}) that is similar to the activities of both human FKBP12 and SlyD from *T. thermophilus*. This illustrates the advantage of a sensitive and robust protease-free assay for prolyl isomerases using doubly labeled peptides. In the protease-free assay, the role of the residue after the proline can, in principle, be varied as well, unlike in the protease-coupled assays, where this residue is used as the recognition site for the protease.

Specificities of Human FKBP12, Cyclophilin 18, and Parvulin 14 Probed by the Protease-Free Assay and the Peptide Library. In the following, we employed our library of Abz peptides, solvent jump experiments, and the protease-free assay to characterize the substrate specificities of human representatives of the three major families of prolyl isomerases: hCyp18 from the cyclophilin family, hFKBP12 from the FKBP family, and hPar14 from the parvulin family. Proteins do not absorb at the excitation wavelength of the Abz group (316 nm),

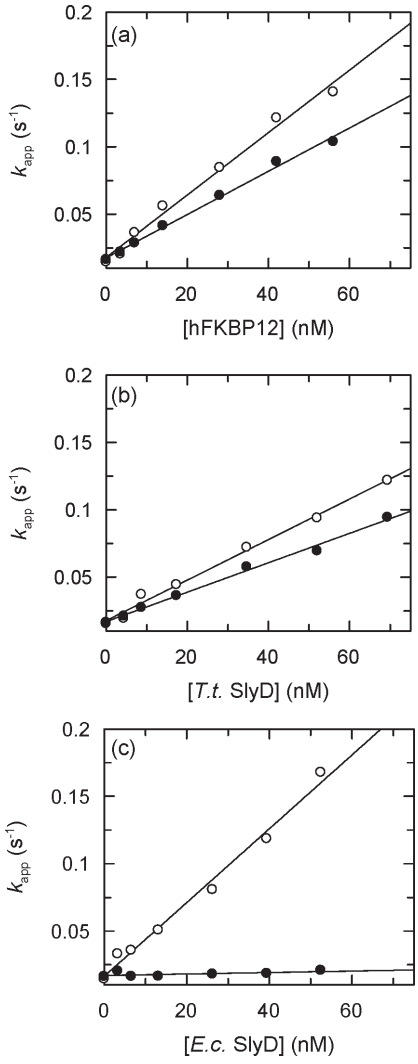

FIGURE 9: Prolyl isomerase activities of (a) hFKBP12, (b) *T. thermophilus* SlyD, and (c) *E. coli* SlyD measured by the protease-coupled assay (●) or the protease-free assay (○) at 15 °C using 2 μM Abz-Ala-Leu-Pro-Phe-pNA peptide. Solvent jumps were initiated by a 200-fold dilution of the peptide (in 0.55 M LiCl/TFE) with 0.1 M potassium phosphate and 1 mM EDTA (pH 7.5). The protease-coupled assay was performed in the presence of 240 μM α-chymotrypsin. Fluorescence at 416 nm was measured after excitation at 316 nm. The time courses of the *cis*−*trans* isomerization were analyzed as single-exponential reactions, and the apparent rate constants are plotted as a function of enzyme concentration. Apparent k_{cat}/K_M values of (a) 1.6 and 2.3×10^6 M^{-1} s^{-1}, (b) 1.1 and 1.5×10^6 M^{-1} s^{-1}, and (c) 2.8×10^6 M^{-1} s^{-1} and zero were obtained for the protease-free and protease-coupled assays, respectively, from the slopes of the lines.

and therefore, high protein concentrations could be employed to characterize prolyl isomerases with very low enzymatic activities.

The activities of the three prolyl isomerases toward the Ala peptide are strongly different and varied by almost 4 orders of magnitude (Figure 10). hCyp18 is highly active, and 13 nM hCyp18 accelerates the isomerization 10-fold (Figure 10a). The catalytic efficiency of hCyp18 is $(8.7 \pm 0.3) \times 10^6$ M^{-1} s^{-1} (Figure 10b). hFKBP12 was ~40-fold less efficient and displayed a catalytic efficiency of $(0.23 \pm 0.20) \times 10^6$ M^{-1} s^{-1} (Figure 10c, d). hPar14 was almost inactive and exhibited a catalytic efficiency of only $(1 \pm 0.1) \times 10^3$ M^{-1} s^{-1} (Figure 10e,f). It was possible to measure this activity, because hPar14 could be employed at high concentrations in this assay.

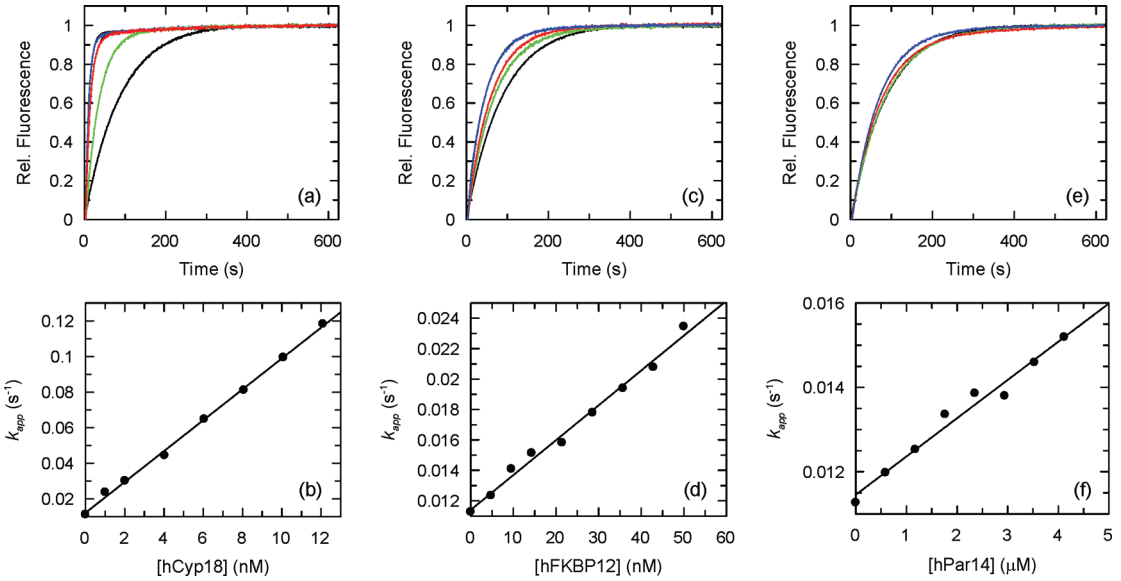

FIGURE 10: Catalysis of the *cis*−*trans* isomerization in Abz-Ala-Ala-Pro-Phe-pNA by different prolyl isomerases. The time course of the reaction is described by the rate constant $k_{app} = k_0 + [E] \times k_{cat}/K_M$, where k_0 is the rate constant of the uncatalyzed reaction, [E] is the enzyme concentration, and k_{cat} and K_M are the turnover number and the Michaelis constant, respectively. (a) Isomerization in the absence (black; $\tau = k_{app}^{-1} = 88$ s) and presence of 2.5 nM (green; $\tau = 33$ s), 8 nM (red; $\tau = 12$ s), and 13 nM hCyp18 (blue; $\tau = 8.5$ s). (b) Dependence of k_{app} on enzyme concentration. The slope yields a k_{cat}/K_M of $(8.69 \pm 0.280) \times 10^6$ M^{-1} s^{-1}. (c) Isomerization in the absence (black; $\tau = 88$ s) and presence of 10 nM (green; $\tau = 64$ s), 20 nM (red; $\tau = 57$ s), and 50 nM hFKBP12 (blue; $\tau = 43$ s). (d) Dependence of k_{app} on enzyme concentration, giving a k_{cat}/K_M of $(0.23 \pm 0.01) \times 10^6$ M^{-1} s^{-1}. (e) Isomerization in the absence (black; $\tau = 88$ s) and presence of 1.2 μM (green; $\tau = 80$ s), 2.4 μM (red; $\tau = 72$ s), and 4.1 μM hPar14 (blue; $\tau = 66$ s). (f) Dependence of k_{app} on enzyme concentration, giving a k_{cat}/K_M of $(0.9 \pm 0.1) \times 10^3$ M^{-1} s^{-1}. All measurements were performed in 50 mM HEPES (pH 7.8) at 15 °C and 3 μM peptide. Fluorescence was measured at 416 nm after excitation at 316 nM.

The catalytic efficiencies of hFKBP12, hCyp18, and hPar14 were then determined for all peptides of the library (Figure 11 and Table S7 of the Supporting Information). hCyp18 exhibited a very high activity coupled with a very low substrate specificity (Figure 11a). The highest efficiency was observed for the Thr−Pro bond (2×10^7 M^{-1} s^{-1}). Weak catalysis was observed only for the peptide in which Pro was preceded by another Pro (the Pro peptide). A similarly low specificity had been observed previously with a restricted set of peptides and the protease-coupled assay (*15*, *55*, *56*). These published values are compared with those for the complete library in Figure S3 of the Supporting Information. Cyclophilin is a highly active prolyl isomerase with a very low specificity toward the amino acid before the proline. An exceptionally low activity was found for Pro−Pro bond isomerization. This explains the marginal effect of cyclophilins on the folding of procollagen I which contains multiple Pro−Pro bonds (*57*).

hFKBP12 is less active but exhibits a much more pronounced specificity toward residue Xaa (Figure 11b). This enzyme catalyzed the isomerization very well when the proline was preceded by a hydrophobic or aromatic amino acid. The highest value was observed for the Leu peptide ($k_{cat}/K_M = 2.3 \times 10^6$ M^{-1} s^{-1}). The catalytic efficiency was strongly decreased when proline was preceded by negatively charged residues or by another proline. The activities of hFKBP12 toward the Asp and Leu peptides differ ~500-fold. The comparison with the limited set of published values can also be found in Figure S3 of the Supporting Information. The catalytic efficiency of hFKBP12 correlates with the calculated hydrophobicity of the side chain as measured by water/octanol transfer free energies [correlation coefficient $r = 0.73$ (Figure S4 of the Supporting Information)] which is in agreement with published data (*15*, *58*). Such a correlation was not found for hCyp18 or hPar14.

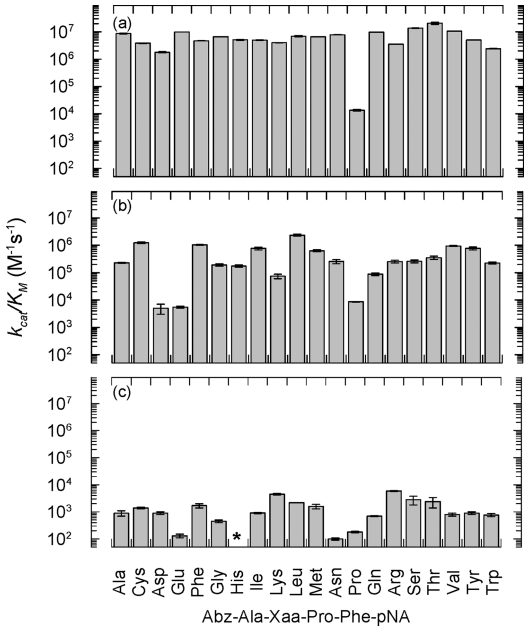

FIGURE 11: Catalytic efficiencies (k_{cat}/K_M) for the *cis*−*trans* isomerization of Abz-Ala-Xaa-Pro-Phe-pNA by (a) hCyp18, (b) hFKBP12, and (c) hPar14. The abscissa shows the identity of residue Xaa in the peptide. The catalytic efficiencies were derived from measurements as shown in Figure 10 for the Ala peptide. The standard deviations were obtained from fits as shown in Figure 10b,d,f. The measurements were performed at 15 °C and pH 7.8 as described in the legend of Figure 10. The asterisk denotes that a catalysis could not be observed for the His peptide, even at 20 μM hPar14.

The catalytic activity of hPar14 is generally extremely low (Figure 11c) and, on average, more than 3 orders of magnitude lower than the corresponding values for hCyp18. In its activity

profile, hPar14 differs from both cyclophilin and FKBP12, and therefore, it appears unlikely that the measured low activities originate from minor impurities in the hPar14 preparation. Also, the activity is not abolished via addition of inhibitors specific for cyclophilin [20 μM cyclosporine A (data not shown)] or FKBP [30 μM FK-506 (data not shown)]. The highest activities ($k_{cat}/K_M \sim 10^4$ M^{-1} s^{-1}) were observed when proline was preceded by a positively charged residue, as in the Lys and Arg peptides. This is consistent with the results obtained previously using the ISP assay (*16*). A catalysis could not be observed for the His peptide, even at 20 μM hPar14.

Catalytic Efficiencies of Different SlyD Proteins. SlyD is a prokaryotic protein that combines a prolyl isomerase function with chaperone properties (*59*−*62*). It consists of a canonical FKBP domain [homologous to hFKBP12 (Figure 1)] and an additional chaperone domain that is inserted into an extended loop (the "flap") near the prolyl isomerase site (*63*). Several SlyD proteins such as the protein from *E. coli* contain unstructured carboxy-terminal extensions that are rich in His and Cys residues and probably involved in Ni^{2+} binding (*64*, *65*). The SlyD proteins from different species are highly active as folding catalysts of a proline-limited refolding reaction, and they exhibited chaperone properties (*25*). Here we employed the library of doubly labeled peptides and the protease-free assay to investigate the catalytic specificity of the SlyD proteins from seven bacteria, i.e., *E. coli* (*Ec*), *Yersinia pestis* (*Yp*), *Treponema pallidum* (*Tp*), *Pasteurella multocida* (*Pm*), *Vibrio cholerae* (*Vc*), *T. thermophilus* (*Tt*), and *Deinococcus radiodurans* (*Dr*).

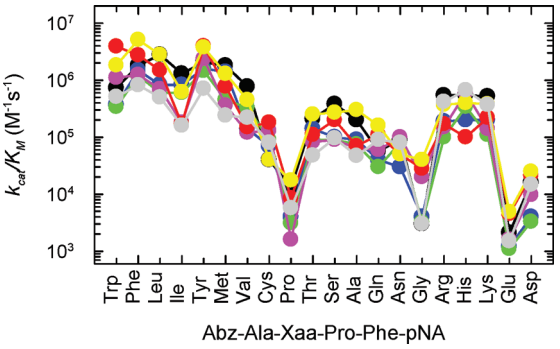

FIGURE 12: Catalytic efficiencies (k_{cat}/K_M) of the SlyD proteins from *E. coli* (black), *Y. pestis* (blue), *Tr. pallidum* (pink), *P. multocida* (green), *V. cholerae* (yellow), *T. thermophilus* (red), and *D. radiodurans* (gray). The abscissa shows the nature of residue Xaa in the peptide. The order of the residues reflects their decreasing hydrophobicity (as measured by transfer free energy from water to octanol for a given residue) (*70*, *71*). The catalytic efficiencies were derived from measurements as described in the legend of Figure 10.

The k_{cat}/K_M values for all peptides and all SlyD homologues are shown in Figure 12 and listed in Table S8 of the Supporting Information. In this plot, the peptides are arranged according to the hydrophobicity of the amino acid before proline in the doubly labeled peptide. Overall, the individual SlyD proteins exhibit similar substrate specificities with very high activities around 10^6 M^{-1} s^{-1} for hydrophobic residues such as Leu, Tyr, and Phe and very low catalytic efficiencies of 10^3−10^4 M^{-1} s^{-1} for Gly, Glu, and Pro. This general pattern confirms that the SlyD proteins are in fact FKBP proteins, as exemplified by the similarity with hFKBP12. The highest catalytic efficiency was found for the Phe peptide (5×10^6 M^{-1} s^{-1} for *Vc* SlyD). Among the SlyD proteins, the differences in catalytic efficiencies for the same substrate varied between 3-fold (Ala peptide) and 13-fold (for Gly peptide). The peptide library and plots such as those in Figure 12 can be used in the future to establish fingerprints for the substrate specificities of prolyl isomerase families.

Conserved Substrate Specificity and Evolution of the FKBP Proteins. The solution three-dimensional structure of *Ec* SlyD is known (*63*), and in the following, we use a structure-based alignment with hFKBP12 to evaluate the sequence differences in the prolyl isomerase active site, between *Ec* SlyD and hFKBP12, as well as between the different SlyD proteins. For hFKBP12, a wealth of mutational data are available that define critical residues in the active-site cavity of the enzyme (Figure 13) (*17*, *55*). Figure S5 of the Supporting Information shows

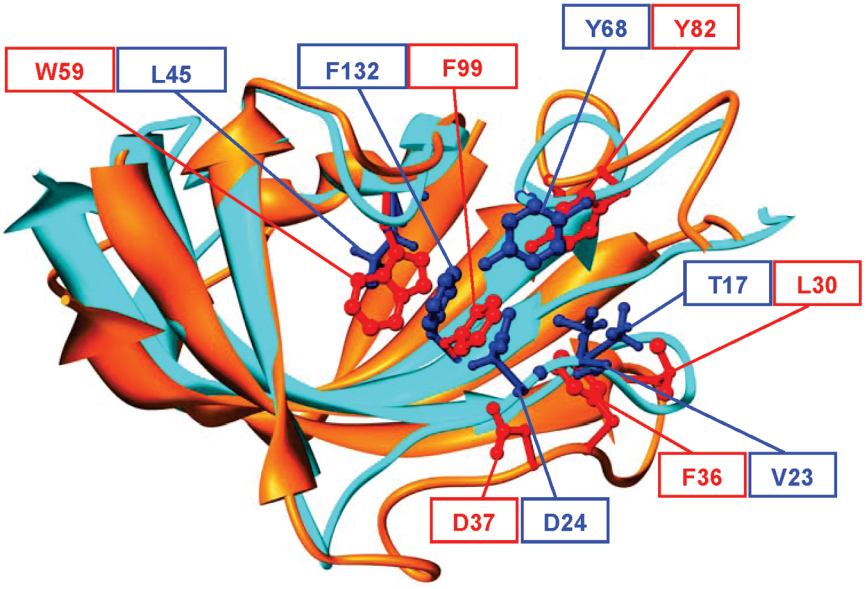

FIGURE 13: Structure-based alignment of the FKBP domains of *E. coli* SlyD (red; PDB entry 2k8i) and hFKBP12 (blue; PDB entry 1fkf). Using the three-dimensional structures, the backbone atoms of the FKBP domains of hFKBP12 (1−109) and SlyD (1−71 and 122−153) were aligned, and this enabled us to find residues at the geometrically equivalent positions. Conserved residues contributing to the enzyme activity (hFKBP12/SlyD, L30/T17, F36/V23, D37/D24, W59/L45, Y82/Y68, and F99/F132) are shown in ball-and-stick representation. The figure was prepared using UCSF Chimera (*69*).

a multiple-sequence alignment of the different bacterial SlyD proteins of this study. SlyD proteins show pairwise sequence identities between 30% (*Dr* vs *Ec*) and 80% (*Ec* vs *Yp*). We use these sequence comparisons and our finding that all these enzymes exhibit similar activities and specificities to draw conclusions about the enzymatic mechanism of these proteins.

The structure alignment between hFKBP12 and *Ec* SlyD (Figure 13) identified residues at spatially equivalent positions. In human FKBP12, no single mutations are known that abolish the prolyl isomerase activity completely. At several positions, however, mutations led to significant decreases in activity. These residues include L30, F36, D37, W59, and F99 (*17*, *55*). Substitutions Y82F and H87L led to slight changes in substrate specificity (*55*). From these residues, only those corresponding to D37, F99, and Y82 of hFKBP12 are conserved at corresponding positions in *Ec* SlyD (Figure 13).

The L30A substitution in the ^{29}MLEDG sequence led to a 5-fold decrease in the catalytic efficiency of hFKBP12. This leucine is replaced with threonine in *Ec* SlyD, but the two neighboring, negatively charged residues are conserved (as ^{16}RTEDG) in most SlyD proteins.

Substitution F36Y decreased the activity of hFKBP12 to 5%. The equivalent position 23 in SlyD is occupied by Val in a stretch of conserved hydrophobic residues (^{21}VLV), which is found in several other SlyD proteins as well. D37 is highly conserved in FKBP proteins and also in *Ec* SlyD (as D24) and in most other SlyD proteins. The W59L substitution decreased the catalytic efficiency of hFKBP12 to 13% (*55*). It is replaced with Leu (L45) in *Ec* SlyD* and all other SlyD proteins, where it forms part of the GLE consensus sequence. Y82 as part of a highly conserved AYG motif is present in hFKBP12 as well as in *Ec* SlyD (as Y68) and most other SlyD proteins. F99 is considered to be the catalytically most important residue in hFKBP12, and the F99L mutation decreased the catalytic efficiency to 0.2% (*55*). This residue occupies a very similar position and is conserved (as F132) in *Ec* SlyD and all other SlyD proteins (Figure 13).

In summary, a high degree of conservation of the substrate specificities between hFKBP12 and SlyD and within the SlyD family is not correlated with a conservation of residues in the active-site region. This suggests that an overall hydrophobic binding pocket might in fact be sufficient to maintain the catalytic activity and the substrate specificities of the FKBP-type prolyl isomerases.

Conclusion. The library of doubly labeled Abz-Ala-Xaa-Pro-Phe-pNA tetrapeptides together with our protease-free fluorescence assay provides a general tool for measuring the activities of prolyl isomerases with high sensitivity and for characterizing their substrate specificities. Here it was used here to elucidate the P1-site specificities for FKBP12, cyclophilin 18, and parvulin 14 and to characterize the substrate specificity of a group of SlyD proteins from different bacteria.

ACKNOWLEDGMENT

We thank Alexandra Thiele and Sebastian Mathea for preparation of hPar14 and hFKBP12 and members of our groups for very helpful discussions. The bacterial SlyD homologues were a generous gift of Dr. Christian Scholz (Roche Diagnostics GmbH, Penzberg, Germany). We thank Dr. Christian Wespe for helpful discussions about the use of ionic liquids. Technical assistance by B. Hökelmann and M. Seidel is gratefully acknowledged.

SUPPORTING INFORMATION AVAILABLE

Six tables and five figures with data on the MD calculations, the NMR experiments, and catalyzed prolyl isomerization. This material is available free of charge via the Internet at http://pubs.acs.org.

REFERENCES

1. Schmid, F. X., Mayr, L. M., Mücke, M., and Schönbrunner, E. R. (1993) Prolyl isomerases: Role in protein folding. *Adv. Protein Chem. 44*, 25–66.
2. Eckert, B., Martin, A., Balbach, J., and Schmid, F. X. (2005) Prolyl isomerization as a molecular timer in phage infection. *Nat. Struct. Mol. Biol. 12*, 619–623.
3. Vogel, M., Bukau, B., and Mayer, M. P. (2006) Allosteric regulation of Hsp70 chaperones by a proline switch. *Mol. Cell 21*, 359–367.
4. Vogel, M., Mayer, M. P., and Bukau, B. (2006) Allosteric regulation of Hsp70 chaperones involves a conserved interdomain linker. *J. Biol. Chem. 281*, 38705–38711.
5. Lu, K. P., Finn, G., Lee, T. H., and Nicholson, L. K. (2007) Prolyl cis-trans isomerization as a molecular timer. *Nat. Chem. Biol. 3*, 619–629.
6. Schutkowski, M., Bernhardt, A., Zhou, X. Z., Shen, M., Reimer, U., Rahfeld, J. U., Lu, K. P., and Fischer, G. (1998) Role of phosphorylation in determining the backbone dynamics of the serine/threonine-proline motif and Pin1 substrate recognition. *Biochemistry 37*, 5566–5575.
7. Sarkar, P., Reichman, C., Saleh, T., Birge, R. B., and Kalodimos, C. G. (2007) Proline cis-trans isomerization controls autoinhibition of a signaling protein. *Mol. Cell 25*, 413–426.
8. Mallis, R. J., Brazin, K. N., Fulton, D. B., and Andreotti, A. H. (2002) Structural characterization of a proline-driven conformational switch within the Itk SH2 domain. *Nat. Struct. Biol. 9*, 900–905.
9. Severin, A., Joseph, R. E., Boyken, S., Fulton, D. B., and Andreotti, A. H. (2009) Proline isomerization preorganizes the Itk SH2 domain for binding to the Itk SH3 domain. *J. Mol. Biol. 387*, 726–743.
10. Yaron, A., and Naider, F. (1993) Proline-dependent structural and biological properties of peptides and proteins. *Crit. Rev. Biochem. Mol. Biol. 28*, 31–81.
11. Göthel, S. F., and Marahiel, M. A. (1999) Peptidyl-prolyl cis-trans isomerases, a superfamily of ubiquitous folding catalysts. *Cell. Mol. Life Sci. 55*, 423–436.
12. Fischer, G., Wittmann-Liebold, B., Lang, K., Kiefhaber, T., and Schmid, F. X. (1989) Cyclophilin and peptidyl-prolyl cis-trans isomerase are probably identical proteins. *Nature 337*, 476–478.
13. Fischer, G., Bang, H., Berger, E., and Schellenberger, A. (1984) Conformational specificity of chymotrypsin toward proline-containing substrates. *Biochim. Biophys. Acta 791*, 87–97.
14. Fischer, G., Bang, H., and Mech, C. (1984) [Determination of enzymatic catalysis for the cis-trans-isomerization of peptide binding in proline-containing peptides]. *Biomed. Biochim. Acta 43*, 1101–1111.
15. Harrison, R. K., and Stein, R. L. (1990) Substrate specificities of the peptidyl prolyl cis-trans isomerase activities of cyclophilin and FK-506 binding protein: Evidence for the existence of a family of distinct enzymes. *Biochemistry 29*, 3813–3816.
16. Uchida, T., Fujimori, F., Tradler, T., Fischer, G., and Rahfeld, J. U. (1999) Identification and characterization of a 14 kDa human protein as a novel parvulin-like peptidyl prolyl cis/trans isomerase. *FEBS Lett. 446*, 278–282.
17. Park, S. T., Aldape, R. A., Futer, O., DeCenzo, M. T., and Livingston, D. J. (1992) PPIase catalysis by human FK506-binding protein proceeds through a conformational twist mechanism. *J. Biol. Chem. 267*, 3316–3324.
18. Lin, L. N., and Brandts, J. F. (1985) Isomer-specific proteolysis of model substrates: Influence that the location of the proline residue exerts on cis/trans specificity. *Biochemistry 24*, 6533–6538.
19. Kofron, J. L., Kuzmic, P., Kishore, V., Colon-Bonilla, E., and Rich, D. H. (1991) Determination of kinetic constants for peptidyl prolyl cis-trans isomerases by an improved spectrophotometric assay. *Biochemistry 30*, 6127–6134.
20. Janowski, B., Wollner, S., Schutkowski, M., and Fischer, G. (1997) A protease-free assay for peptidyl prolyl cis/trans isomerases using standard peptide substrates. *Anal. Biochem. 252*, 299–307.

21. Garcia-Echeverria, C., Kofron, J. L., Kuzmic, P., Kishore, V., and Rich, D. H. (1992) Continuous fluorometric direct (uncoupled) assay for peptidyl prolyl cis-trans isomerases. *J. Am. Chem. Soc. 114*, 2758–2759.
22. Garcia-Echeverria, C., Kofron, J. L., Kuzmic, P., and Rich, D. H. (1993) A continuous spectrophotometric direct assay for peptidyl prolyl cis-trans isomerases. *Biochem. Biophys. Res. Commun. 191*, 70–75.
23. Schiene, C., Reimer, U., Schutkowski, M., and Fischer, G. (1998) Mapping the stereospecificity of peptidyl prolyl cis/trans isomerases. *FEBS Lett. 432*, 202–206.
24. Liu, J., Albers, M. W., Chen, C. M., Schreiber, S. L., and Walsh, C. T. (1990) Cloning, expression, and purification of human cyclophilin in *Escherichia coli* and assessment of the catalytic role of cysteines by site-directed mutagenesis. *Proc. Natl. Acad. Sci. U.S.A. 87*, 2304–2308.
25. Scholz, C., Eckert, B., Hagn, F., Schaarschmidt, P., Balbach, J., and Schmid, F. X. (2006) SlyD proteins from different species exhibit high prolyl isomerase and chaperone activities. *Biochemistry 45*, 20–33.
26. Tradler, T., Stoller, G., Rücknagel, K. P., Schierhorn, A., Rahfeld, J. U., and Fischer, G. (1997) Comparative mutational analysis of peptidyl prolyl cis/trans isomerases: active sites of *Escherichia coli* trigger factor and human FKBP12. *FEBS Lett. 407*, 184–190.
27. Barlos, K., Gatos, D., Kallitsis, J., Papaphotiu, G., Sotiriu, P., Yao, W. Q., and Schafer, W. (1989) Synthesis of Protected Peptide-Fragments Using Substituted Triphenylmethyl Resins. *Tetrahedron Lett. 30*, 3943–3946.
28. Bollhagen, R., Schmiedberger, M., Barlos, K., and Grell, E. (1994) A New Reagent for the Cleavage of Fully Protected Peptides Synthesized on 2-Chlorotrityl Chloride Resin. *J. Chem. Soc., Chem. Commun.,* 2559–2560.
29. Boens, N., Qin, W. W., Basaric, N., Hofkens, J., Ameloot, M., Pouget, J., Lefevre, J. P., Valeur, B., Gratton, E., Vandeven, M., Silva, N. D., Engelborghs, Y., Willaert, K., Sillen, A., Rumbles, G., Phillips, D., Visser, A. J. W. G., van Hoek, A., Lakowicz, J. R., Malak, H., Gryczynski, I., Szabo, A. G., Krajcarski, D. T., Tamai, N., and Miura, A. (2007) Fluorescence lifetime standards for time and frequency domain fluorescence spectroscopy. *Anal. Chem. 79*, 2137–2149.
30. Lakowicz, J. R. (1999) Principles of Fluorescence Spectroskopy, Kluwer Academic/Plenum Publishers, New York.
31. Delmar, E. G., Largman, C., Brodrick, J. W., and Geokas, M. C. (1979) Sensitive New Substrate for Chymotrypsin. *Anal. Biochem. 99*, 316–320.
32. Stryer, L. (1978) Fluorescence Energy-Transfer as a Spectroscopic Ruler. *Annu. Rev. Biochem. 47*, 819–846.
33. Wishart, D. S., Bigam, C. G., Holm, A., Hodges, R. S., and Sykes, B. D. (1995) ^{1}H, ^{13}C and ^{15}N random coil NMR chemical shifts of the common amino acids. I. Investigations of nearest-neighbor effects. *J. Biomol. NMR 5*, 67–81.
34. Wishart, D. S., Bigam, C. G., Yao, J., Abildgaard, F., Dyson, H. J., Oldfield, E., Markley, J. L., and Sykes, B. D. (1995) ^{1}H, ^{13}C and ^{15}N chemical shift referencing in biomolecular NMR. *J. Biomol. NMR 6*, 135–140.
35. Molecular Operating Environment (2008) Chemical Computing Group Inc. Montreal, Canada.
36. Christen, M., Hünenberger, P. H., Bakowies, D., Baron, R., Burgi, R., Geerke, D. P., Heinz, T. N., Kastenholz, M. A., Krautler, V., Oostenbrink, C., Peter, C., Trzesniak, D., and Van Gunsteren, W. F. (2005) The GROMOS software for biomolecular simulation: GROMOS05. *J. Comput. Chem. 26*, 1719–1751.
37. Oostenbrink, C., Villa, A., Mark, A. E., and Van Gunsteren, W. F. (2004) A biomolecular force field based on the free enthalpy of hydration and solvation: The GROMOS force-field parameter sets 53A5 and 53A6. *J. Comput. Chem. 25*, 1656–1676.
38. Ryckaert, J. P., Ciccotti, G., and Berendsen, H. J. C. (1977) Numerical-Integration of Cartesian Equations of Motion of a System with Constraints: Molecular-Dynamics of N-Alkanes. *J. Comput. Phys. 23*, 327–341.
39. Hockney, R. W. (1970) The potential calculations and some applications. *Methods Comput. Phys. 9*, 136–211.
40. Berendsen, H. J. C., Postma, J. P. M., van Gunsteren, W. F., DiNola, A., and Haak, J. R. (1984) Molecular dynamics with coupling to an external bath. *J. Chem. Phys. 81*, 3684–3690.
41. Berendsen, H. J. C., Postma, J. P. M., van Gunsteren, W. F., and Hermans, J. (1981) Interaction models for water in relation to protein hydration. In Intermolecular Forces , pp 331−342.
42. Tironi, I. G., Sperb, R., Smith, P. E., and van Gunsteren, W. F. (1995) A generalized reaction field method for molecular-dynamics simulations. *J. Chem. Phys. 102*, 5451–5459.
43. Daura, X., van Gunsteren, W. F., and Mark, A. E. (1999) Folding-unfolding thermodynamics of a β-heptapeptide from equilibrium simulations. *Proteins: Struct., Funct., Genet. 34*, 269–280.
44. Wüthrich, K. (1986) in NMR of Proteins and Nucleic Acids, Wiley, New York.
45. Schubert, M., Labudde, D., Oschkinat, H., and Schmieder, P. (2002) A software tool for the prediction of Xaa-Pro peptide bond conformations in proteins based on ^{13}C chemical shift statistics. *J. Biomol. NMR 24*, 149–154.
46. Yaron, A., Carmel, A., and Katchalski-Katzir, E. (1979) Intramolecularly quenched fluorogenic substrates for hydrolytic enzymes. *Anal. Biochem. 95*, 228–235.
47. Wehofsky, N., Wespe, C., Cerovsky, V., Pech, A., Hoess, E., Rudolph, R., and Bordusa, F. (2008) Ionic liquids and proteases: A clean alliance for semisynthesis. *ChemBioChem 9*, 1493–1499.
48. Reimer, U., Scherer, G., Drewello, M., Kruber, S., Schutkowski, M., and Fischer, G. (1998) Side-chain effects on peptidyl-prolyl cis/trans isomerisation. *J. Mol. Biol. 279*, 449–460.
49. Jakob, R. P., and Schmid, F. X. (2009) Molecular determinants of a native-state prolyl isomerization. *J. Mol. Biol. 387*, 1017–1031.
50. Bernhardt, T. G., Roof, W. D., and Young, R. (2002) The *Escherichia coli* FKBP-type PPIase SlyD is required for the stabilization of the E lysis protein of bacteriophage phi X174. *Mol. Microbiol. 45*, 99–108.
51. Hottenrott, S., Schumann, T., Plückthun, A., Fischer, G., and Rahfeld, J. U. (1997) The *Escherichia coli* SlyD is a metal ion-regulated peptidyl-prolyl cis/trans-isomerase. *J. Biol. Chem. 272*, 15697–15701.
52. Roof, W. D., Fang, H. Q., Young, K. D., Sun, J., and Young, R. (1997) Mutational analysis of slyD, an *Escherichia coli* gene encoding a protein of the FKBP immunophilin family. *Mol. Microbiol. 25*, 1031–1046.
53. Roof, W. D., Horne, S. M., Young, K. D., and Young, R. (1994) slyD, a host gene required for phi X174 lysis, is related to the FK506-binding protein family of peptidyl-prolyl cis-trans-isomerases. *J. Biol. Chem. 269*, 2902–2910.
54. Roof, W. D., and Young, R. (1995) Phi X174 lysis requires slyD, a host gene which is related to the FKBP family of peptidyl-prolyl cis-trans isomerases. *FEMS Microbiol. Rev. 17*, 213–218.
55. DeCenzo, M. T., Park, S. T., Jarrett, B. P., Aldape, R. A., Futer, O., Murcko, M. A., and Livingston, D. J. (1996) FK506-binding protein mutational analysis: Defining the active-site residue contributions to catalysis and the stability of ligand complexes. *Protein Eng. 9*, 173–180.
56. Albers, M. W., Walsh, C. T., and Schreiber, S. L. (1990) Substrate specificity for the human Rotamase FKBP: A view of FK506 and rapamycin as leucin-(twisted amide)-proline mimics. *J. Org. Chem. 55*, 4984–4986.
57. Steinmann, B., Bruckner, P., and Superti-Furga, A. (1991) Cyclosporin A slows collagen triple-helix formation in vivo: Indirect evidence for a physiologic role of peptidyl-prolyl cis-trans-isomerase. *J. Biol. Chem. 266*, 1299–1303.
58. Kramer, M. L., and Fischer, G. (1997) FKBP-like catalysis of peptidyl-prolyl bond isomerization by micelles and membranes. *Biopolymers 42*, 49–60.
59. Han, K. Y., Song, J. A., Ahn, K. Y., Park, J. S., Seo, H. S., and Lee, J. (2007) Solubilization of aggregation-prone heterologous proteins by covalent fusion of stress-responsive *Escherichia coli* protein, SlyD. *Protein. Eng., Des. Sel. 20*, 543–549.
60. Knappe, T. A., Eckert, B., Schaarschmidt, P., Scholz, C., and Schmid, F. X. (2007) Insertion of a chaperone domain converts FKBP12 into a powerful catalyst of protein folding. *J. Mol. Biol. 368*, 1458–1468.
61. Scholz, C., Schaarschmidt, P., Engel, A. M., Andres, H., Schmitt, U., Faatz, E., Balbach, J., and Schmid, F. X. (2005) Functional solubilization of aggregation-prone HIV envelope proteins by covalent fusion with chaperone modules. *J. Mol. Biol. 345*, 1229–1241.
62. Scholz, C., Thirault, L., Schaarschmidt, P., Zarnt, T., Faatz, E., Engel, A. M., Upmeier, B., Bollhagen, R., Eckert, B., and Schmid, F. X. (2008) Chaperone-aided in vitro renaturation of an engineered E1 envelope protein for detection of anti-Rubella virus IgG antibodies. *Biochemistry 47*, 4276–4287.
63. Weininger, U., Haupt, C., Schweimer, K., Graubner, W., Kovermann, M., Brüser, T., Scholz, C., Schaarschmidt, P., Zoldak, G., Schmid, F. X., and Balbach, J. (2009) NMR solution structure of SlyD from *Escherichia coli*: Spatial separation of prolyl isomerase and chaperone function. *J. Mol. Biol. 387*, 295–305.

64. Leach, M. R., Zhang, J. W., and Zamble, D. B. (2007) The role of complex formation between the *Escherichia coli* hydrogenase accessory factors HypB and SlyD. *J. Biol. Chem. 282*, 16177–16186.
65. Mitterauer, T., Nanoff, C., Ahorn, H., Freissmuth, M., and Hohenegger, M. (1999) Metal-dependent nucleotide binding to the *Escherichia coli* rotamase SlyD. *Biochem. J. 342* (Part 1), 33–39.
66. Ottiger, M., Zerbe, O., Guntert, P., and Wüthrich, K. (1997) The NMR solution conformation of unligated human cyclophilin A. *J. Mol. Biol. 272*, 64–81.
67. Van Duyne, G. D., Standaert, R. F., Karplus, P. A., Schreiber, S. L., and Clardy, J. (1991) Atomic structure of FKBP-FK506, an immunophilin-immunosuppressant complex. *Science 252*, 839–842.
68. Terada, T., Shirouzu, M., Fukumori, Y., Fujimori, F., Ito, Y., Kigawa, T., Yokoyama, S., and Uchida, T. (2001) Solution structure of the human parvulin-like peptidyl prolyl cis/trans isomerase, hPar14. *J. Mol. Biol. 305*, 917–926.
69. Pettersen, E. F., Goddard, T. D., Huang, C. C., Couch, G. S., Greenblatt, D. M., Meng, E. C., and Ferrin, T. E. (2004) UCSF Chimera: A visualization system for exploratory research and analysis. *J. Comput. Chem. 25*, 1605–1612.
70. Fauchere, J., and Pliska, V. (1983) Hydrophobic parameters p of aminoacid side chains from the partitioning of N-acetyl-amino-acid-amides. *Eur. J. Med. Chem. 18*, 369–375.
71. Wimley, W. C., Creamer, T. P., and White, S. H. (1996) Solvation energies of amino acid side chains and backbone in a family of host-guest pentapeptides. *Biochemistry 35*, 5109–5124.
72. Krieger, F., Möglich, A., and Kiefhaber, T. (2005) Effect of proline and glycine residues on dynamics and barriers of loop formation in polypeptide chains. *J. Am. Chem. Soc. 127*, 3346–3352.